IEEE Access
Multidisciplinary | Rapid Review | Open Access Journal

Received August 19, 2020, accepted September 1, 2020, date of publication September 18, 2020,
date of current version September 30, 2020.

Digital Object Identifier 10.1109/ACCESS.2020.3024736

Single- and Two-Phase Open-Circuit Fault Tolerant Control for Dual Three-Phase PM Motor Without Phase Shifting

ZHUOHANG LI, LIJIAN WU, (Senior Member, IEEE), ZEKAI CHEN, YANG SHI, LIN QIU, (Member, IEEE), AND YOUTONG FANG, (Senior Member, IEEE)
College of Electrical Engineering, Zhejiang University, Hangzhou 310027, China

Corresponding authors: Lijian Wu (ljw@zju.edu.cn) and Yang Shi (shiy2@zju.edu.cn)

This work was supported in part by the National Key Research and Development Program of China under Grant 2018YFB1501304, and in part by the National Natural Science Foundation of China under Grant 51677169, Grant 51637009, and Grant 51827810.

ABSTRACT A fault tolerant control strategy for dual three-phase permanent magnet synchronous motor (DTP-PMSM) with 0° phase shifting between two windings is proposed in this paper. When a DTP-PMSM suffers from single- or two-phase open-circuit fault, to maintain the torque performance, current in faulty phase must be compensated by other healthy phases, which causes asymmetric self- and mutual inductances. Therefore, the 2nd harmonic component can be observed in the *dq*-axis currents and torque ripple also increases. To analyse this harmonic component in two types of faults, post-fault model of no-phase-shifting DTP-PMSM based on vector space decomposition (VSD) method is built in this paper. Then, proportion-integral-resonant (PIR) controller which can be used to suppress the specific periodic disturbance is applied to compensate the 2nd harmonic components. As the resonant controller is rarely dependent on motor parameters, phase and amplitude of current harmonic, the PIR controller can be applied in no-phase-shifting DTP-PMSM to suppress the harmonic caused by single- and two-phase open-circuit faults. The experimental results validate the effectiveness of the proposed fault tolerant control under single- and two-phase open-circuit faulty conditions.

INDEX TERMS Dual three-phase, fault tolerant control, harmonic suppression, vector control.

I. INTRODUCTION

Multiphase machines are widely used in industrial applications such as aerospace and traffic because of excellent fault tolerant ability which ensures multiphase machines to work reliably. One of the most studied and applied multiphase machines is the dual three-phase permanent-magnet synchronous motor (DTP-PMSM). A DTP-PMSM contains two sets of armature windings with a specific angle of phase shifting. DTP-PMSMs with 30° phase shifting between two sets of windings [1], [2] were widely researched. However, DTP-PMSMs with 0° phase shifting [3]–[5] obtaining high winding factor and weak coupling between two set of windings [4], [5] were rarely studied in previous research.

Vector space decomposition (VSD) method decoupling torque-producing and flux-producing components achieves high dynamic torque performance, so it was widely used for DTP-PMSMs with 30° phase shifting [6]–[8]. However, it cannot be applied to DTP motors with 0° phase shifting because fundamental and harmonic sub-planes transformed by VSD method are dependent in these motors. Another control method widely used for DTP-PMSMs is the two-individual current control method [9], [10], in which two sets of windings are controlled separately. This control method works properly under healthy condition, especially for DTP-PMSM with 0° phase shifting, since the mutual inductances between two sets of windings are small. However, for multiphase motors, the possibility of failures including open- and short-circuit faults increases with more power devices [11]. When these faults occur, this method is only suitable for DTP-PMSMs with 30° phase shifting [12], while it is unsuitable for DTP-PMSMs with 0° phase shifting because two sets of windings are in phase. Therefore, the VSD method should be modified to be suited for DTP-PMSMs with 0° phase shifting under both healthy and faulty conditions.

The associate editor coordinating the review of this manuscript and approving it for publication was Hao Luo.

An additional leg was applied in [13] to maintain the torque performance under faulty condition, but the topological structure of the driver is complicated and neutral points of the motor must be led out. Therefore, another feasible method is connecting two neutral points [14], and then the current in faulty phase can be compensated by currents in another set of windings. In this way, no additional hardware is introduced in driver system. The latter method is exploited in this paper.

However, this method causes the unbalanced currents between two sets of windings, which leads to asymmetric self- and mutual inductances. The asymmetric inductances cause harmonic disturbance in the *dq*-axis currents. The harmonic components of current and torque in multiphase motors were analysed in [15]–[20]. Harmonic components in the *dq*-axis currents under open-circuit fault mainly contain the 2nd harmonic caused by unbalance inductances [15], [16]. Other harmonics such as the 4th harmonic [17] and the 6th harmonic [19], [20] were analysed separately. However, the harmonics of DTP-PMSM with 0° phase shifting under faulty condition are lack of researching in literature. To suppress current harmonics and torque ripple, the virtual synchronous reference frame method [16], the feedforward compensation method [18] or the genetic algorithm [21] were introduced in fault tolerant control method.

In multiphase motors, the single- and two-phase open-circuit fault tolerant control methods were widely researched [11]. These different types of open-circuit fault can occur on any phase. Therefore, the virtual synchronous reference frame method and the feedforward compensation method which are related to the phase and amplitude of current harmonics need be modified under different open-circuit faulty conditions. Meanwhile, the inaccurate motor inductance measurement can influence the performance of current harmonic suppression in the feedforward compensation method or the genetic algorithm. However, the proportion-integral-resonant (PIR) controller [22], [23] can suppress the periodic disturbance and obtains strong robustness which means that the performance of the PIR controller is barely affected by the phase and amplitude of the current harmonics. The PIR controller can be employed into current loop of vector control [24], [25] and suppress the current harmonic under different open-circuit faulty conditions. However, it lacks research in no-phase-shifting DTP-PMSM fault tolerant control. Therefore, in this paper, the PIR controller is applied in DTP-PMSM with 0° phase shifting fault tolerant control to suppress the current harmonics and torque ripple caused by single- and two-phase open-circuit faults.

In this paper, single- and two-phase open-circuit fault tolerant control strategy for no-phase-shifting DTP-PMSM is proposed. Firstly, in Section II, a new decoupling method based on VSD method is established and then, pre- and post-fault models are built. The 2nd harmonic components are revealed in the post-fault model. Meanwhile, the currents in healthy phase which should be modified to maintain the total magnetic motive force (MMF) under faulty conditions are deduced in Section III. The modification of currents causes asymmetric inductance and leads to the 2nd harmonic *dq*-axis currents which are suppressed by the PIR controller in Section IV. The comparison between the feedforward compensation method and the PIR controller is provided to show the effectiveness and advantage of the PIR controller. Finally, experimental results are provided to demonstrate that the proposed fault tolerant control is effective under single- and two-phase open-circuit faulty conditions.

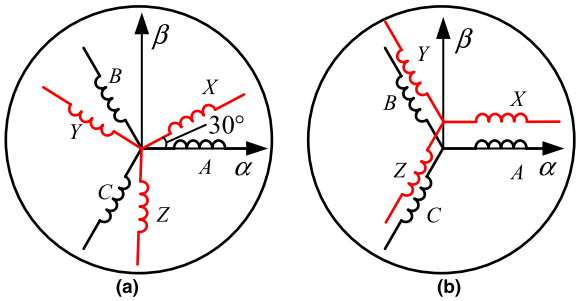

FIGURE 1. Structures of motor windings. (a) Motor with 30° phase shifting between two sets of windings, (b) Motor with 0° phase shifting between two sets of windings.

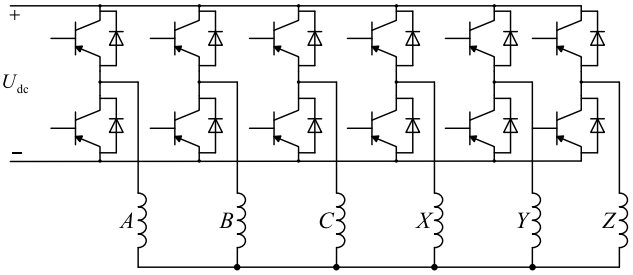

FIGURE 2. Drive system topology.

II. MACHINE MATHEMATICAL MODEL

A. MODEL UNDER ORIGINAL REFERENCE FRAME

The structure of windings and drive system topology of DTP-PMSM with 0° phase shifting are shown in Fig. 1(b) and Fig. 2, respectively, where six phases are named as phase *A, B, C, X, Y, Z*. Phases *A* and *X*, phases *B* and *Y*, phases *C* and *Z* are correspondingly in phase, so the model in the original reference frame can be expressed as:

$$\boldsymbol{u}_s = \boldsymbol{R}_s \boldsymbol{i}_s + \mathrm{d}\boldsymbol{\psi}_s / \mathrm{d}t \tag{1}$$

$$\boldsymbol{\psi}_s = \boldsymbol{L}_s \boldsymbol{i}_s + \boldsymbol{\psi}_{fm} \tag{2}$$

where $\boldsymbol{u}_s = [u_A\ u_B\ u_C\ u_X\ u_Y\ u_Z]^{\mathrm{T}}$ represents the terminal voltage vector of six phases, $\boldsymbol{i}_s$ and ψ_s, similar to $\boldsymbol{u}_s$, represent the current and flux linkage vectors, $\boldsymbol{R}_s$, $\boldsymbol{L}_s$ and ψ_{fm} represent the resistance, inductance and PM flux linkage matrix of six phases, respectively, and [5]

$$\boldsymbol{L}_s = \begin{bmatrix} \boldsymbol{L}_{11} & \boldsymbol{L}_{12} \\ \boldsymbol{L}_{12} & \boldsymbol{L}_{11} \end{bmatrix} = \begin{bmatrix} \boldsymbol{L}_{11} & 2\boldsymbol{L}_0 - \boldsymbol{L}_{11} \\ 2\boldsymbol{L}_0 - \boldsymbol{L}_{11} & \boldsymbol{L}_{11} \end{bmatrix} \tag{3}$$

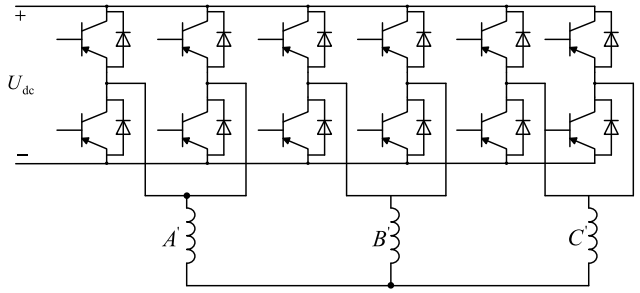

FIGURE 3. Equivalent drive system topology.

where

$$\boldsymbol{L}_{11}=\begin{bmatrix} L_1 & M_2 & M_1 \\ M_2 & L_1 & M_1 \\ M_1 & M_1 & L_1 \end{bmatrix},\quad \boldsymbol{L}_0=\begin{bmatrix} L_0 & M_0 & M_0 \\ M_0 & L_0 & M_0 \\ M_0 & M_0 & L_0 \end{bmatrix} \tag{4}$$

where L_1 represents the phase self-inductance, M_1, M_2 represent the mutual inductances in one set of windings.

Two sets of individual windings can be parallel connected considering that the phase shifting between two sets of windings is 0°. In this way, the DTP-PMSM is equivalent to a single three-phase PMSM and the drive system topology is shown in Fig. 3. The three phases of equivalent PMSM are defined as phase *A*', *B*' and *C*'. The equivalent inductance matrix is $\boldsymbol{L}_0$. Flux linkage of the parallel windings can be calculated by the average of two individual windings, which can be written as:

$$\boldsymbol{\psi}_0=\left(\boldsymbol{\psi}_{11}+\boldsymbol{\psi}_{12}\right)/2 \tag{5}$$

The inductance relationship between the inductance of the parallel windings and individual windings can be derived as:

$$\boldsymbol{L}_0=\left(\boldsymbol{L}_{11}+\boldsymbol{L}_{12}\right)/2 \tag{6}$$

The equivalent PMSM will be further used to analyse the 2nd harmonic in faulty model.

B. PROPOSED VECTOR DECOUPLING METHOD

The transformation matrix of the VSD method can be written as (7), shown at the bottom of the page, where φ represents the phase shifting between two windings.

The matrix transforms the six-phase components into the fundamental and harmonic components. However, φ is equal to zero in DTP-PMSMs with 0° phase shifting and this transformation matrix is unsuitable since the vector α is dependent on the vector z_1, which means that the fundamental and harmonic components are not decoupled.

Therefore, a modified vector decoupling method suitable for DTP-PMSMs with 0° phase shifting is proposed. The fundamental components related to torque performance are deduced from VSD method. The rest components can be defined as unbalanced components which represent the unbalance between two sets of windings. The transformation matrix can be expressed as:

$$\boldsymbol{T}_{6s}=\begin{bmatrix} \boldsymbol{\alpha} \\ \boldsymbol{\beta} \\ z_0 \\ z_1 \\ z_2 \\ z_3 \end{bmatrix}=\frac{1}{3}\begin{bmatrix} 1 & -1/2 & -1/2 & 1 & -1/2 & -1/2 \\ 0 & \sqrt{3}/2 & -\sqrt{3}/2 & 0 & \sqrt{3}/2 & -\sqrt{3}/2 \\ 1 & 1 & 1 & 1 & 1 & 1 \\ 1 & 0 & 0 & -1 & 0 & 0 \\ 0 & 1 & 0 & 0 & -1 & 0 \\ 0 & 0 & 1 & 0 & 0 & -1 \end{bmatrix} \tag{8}$$

The currents of the α-β sub-plane produce rotating MMF and participate in electromechanical energy conversion. The z_0 component is zero-order component. The unbalanced components z_1 represent the unbalance between phase *A* and *X*, which are in phase. The unbalanced components z_2 and z_3 can be defined in the same way. These components are used to solve current sharing problem, but they do not participate in energy conversion. A rotation transformation matrix is used to convert the α-β components to the synchronous reference frame *d*-*q* components whereas the unbalanced components remain unchanged. The transformation matrix can be written as:

$$\boldsymbol{T}_{6r}=\begin{bmatrix} \cos\theta & \sin\theta & 0 \\ -\sin\theta & \cos\theta & 0 \\ 0 & 0 & \boldsymbol{I}_4 \end{bmatrix}\boldsymbol{T}_{6s} \tag{9}$$

The fundamental and unbalanced components are decoupled under healthy condition. The 2nd harmonic components do not exist in the *dq*-axis currents theoretically. The voltage and electromagnetic equations are expressed as:

$$\begin{aligned}\boldsymbol{u}_{dq}=&\,2\left(L_0-M_0\right)\boldsymbol{I}_{2\times2}\frac{d\boldsymbol{i}_{dq}}{dt}+R_s\boldsymbol{I}_{2\times2}\boldsymbol{i}_{dq}\\&-\omega\begin{bmatrix} 0 & 2\left(L_0-M_0\right) \\ -2\left(L_0-M_0\right) & 0 \end{bmatrix}\boldsymbol{i}_{dq}+\omega\psi_{fd}\begin{bmatrix} 0 \\ 1 \end{bmatrix}\end{aligned} \tag{10}$$

$$\begin{bmatrix} \boldsymbol{\alpha} \\ \boldsymbol{\beta} \\ z_1 \\ z_2 \\ \boldsymbol{o}_1 \\ \boldsymbol{o}_2 \end{bmatrix}=\frac{1}{3}\begin{bmatrix} 1 & \cos\left(2\pi/3\right) & \cos\left(4\pi/3\right) & \cos\varphi & \cos\left(2\pi/3+\varphi\right) & \cos\left(4\pi/3+\varphi\right) \\ 0 & -\sin\left(2\pi/3\right) & -\sin\left(4\pi/3\right) & -\sin\varphi & -\sin\left(2\pi/3+\varphi\right) & -\sin\left(4\pi/3+\varphi\right) \\ 1 & \cos\left(4\pi/3\right) & \cos\left(8\pi/3\right) & \cos(2\varphi) & \cos\left(4\pi/3+\varphi\right) & \cos\left(8\pi/3+\varphi\right) \\ 0 & -\sin\left(4\pi/3\right) & -\sin\left(8\pi/3\right) & -\sin(2\varphi) & -\sin\left(4\pi/3+\varphi\right) & -\sin\left(8\pi/3+\varphi\right) \\ 1 & 1 & 1 & 0 & 0 & 0 \\ 0 & 0 & 0 & 1 & 1 & 1 \end{bmatrix} \tag{7}$$

where $\boldsymbol{I}_{2\times2}$ represents the 2nd order identity matrix.

$$\boldsymbol{u}_z = 2\begin{bmatrix} L_1-L_0 & M_2-M_0 & M_1-M_0 \\ M_2-M_0 & L_1-L_0 & M_1-M_0 \\ M_1-M_0 & M_1-M_0 & L_1-L_0 \end{bmatrix}\frac{d\boldsymbol{i}_z}{dt} + R_s\boldsymbol{I}_{3\times3}\boldsymbol{i}_z \tag{11}$$

$$T_e = 1.5p\left(\psi_d i_q - \psi_q i_d\right) \tag{12}$$

where p is the number of pole pairs.

As shown in (11), the components within unbalanced components are not decoupled, which means that one unbalanced component can affect others. However, they cannot affect the fundamental components, and hence the torque performance is immune to the unbalanced components.

C. MODEL UNDER FAULTY CONDITION

The fundamental components are coupled with unbalanced components when the DTP-PMSM suffers from open-circuit fault. The $\alpha\beta$-axis self-inductances under healthy condition are constant and equal due to the non-salient rotor structure, whereas they are asymmetric under open-circuit faulty condition. As a consequence, when they are transformed into the dq-axis self-inductances, the 2nd harmonic components appear. By way of example, this paper assumes that phase A is open-circuit under single-phase faulty condition and phases A and B are open-circuit under two-phase faulty condition, while the conclusion is generally applicable.

The flux linkage of the equivalent single three-phase motor based on (5) can be written as:

$$\psi_{A'} = (\psi_A + \psi_X)/2 = L_0 i_{A'} + M_0 i_{B'} + M_0 i_{C'} + \psi_{fm}\cos\theta \tag{13}$$

where $\psi_{A'}$ represents the flux linkage of equivalent three phase motor, $i_{A'}$, $i_{B'}$, $i_{C'}$ represent the three phase currents of equivalent motor, respectively, and $i_{A'} = i_A + i_X$, $i_{B'} = i_B + i_Y$, $i_{C'} = i_C + i_Z$. $\psi_{B'}$ and $\psi_{C'}$ can be deduced similarly.

When single-phase open-circuit fault occurs, $i_A = 0$ and $\psi_{A'} = \psi_X$. The flux linkage of the equivalent three phase PMSM can be expressed as:

$$\psi_{A'} = (2M_0 - M_2)\, i_B + (2M_0 - M_1)\, i_C + L_1 i_X + M_2 i_Y + M_1 i_Z + \psi_{fm}\cos\theta \tag{14}$$

$$\psi_{B'} = M_0 i_{A'} + L_0 i_{B'} + M_0 i_{C'} + \psi_{fm}\cos\left(\theta - 2\pi/3\right) \tag{15}$$

$$\psi_{C'} = M_0 i_{A'} + M_0 i_{B'} + L_0 i_{C'} + \psi_{fm}\cos\left(\theta + 2\pi/3\right) \tag{16}$$

The inductances in each set of windings are asymmetric shown in (3). However, the inductances of equivalent PMSM are symmetric because the coupling between two sets of windings compensates the asymmetric inductances, and the symmetrical inductances in equivalent PMSM obtains only when currents in two sets of windings are symmetrical. Thus, the equivalent inductance can be affected by current distribution in two sets of windings. When current amplitudes of phase B, C, Y, Z are equal as these current amplitudes under healthy condition, the self-inductance of phases B' and C' and mutual inductance in equivalent motor are unchanged, while self-inductance of phase A' changes to L_1 which is the phase self-inductance of DTP-PMSM. The matrix of flux linkage can be expressed as:

$$\begin{bmatrix}\psi_{A'}\\ \psi_{B'}\\ \psi_{C'}\end{bmatrix} = \begin{bmatrix} L_1 & M_0 & M_0 \\ M_0 & L_0 & M_0 \\ M_0 & M_0 & L_0 \end{bmatrix}\begin{bmatrix} i_{A'}\\ i_{B'}\\ i_{C'}\end{bmatrix} + \psi_{fm}\begin{bmatrix}\cos\theta\\ \cos\left(\theta - 2\pi/3\right)\\ \cos\left(\theta + 2\pi/3\right)\end{bmatrix} \tag{17}$$

The single-phase open-circuit fault causes asymmetric self-inductance in equivalent motor shown in (17). The voltage equation of the dq-axis is expressed in (27), where L represents the α-axis self-inductance under healthy condition and equals to $2(L_0 - M_0)/3$, ΔL represents the asymmetric self-inductance and equals to $2(L_1 - L_0)/3$, R_s represents the stator resistance, ω, θ and Ψ_{fd} represent the electric angular velocity, electric angle of the rotor position and the flux linkage of PM, respectively.

The equivalent PMSM flux linkage equation under two-phase-open-circuit fault condition can be deduced as:

$$\begin{bmatrix}\psi_{A'}\\ \psi_{B'}\\ \psi_{C'}\end{bmatrix} = \begin{bmatrix} L_1 & M_2 & M_0 \\ M_2 & L_1 & M_0 \\ M_0 & M_0 & L_0 \end{bmatrix}\begin{bmatrix} i_{A'}\\ i_{B'}\\ i_{C'}\end{bmatrix} + \psi_{fm}\begin{bmatrix}\cos\theta\\ \cos\left(\theta - 2\pi/3\right)\\ \cos\left(\theta + 2\pi/3\right)\end{bmatrix} \tag{18}$$

The equivalent PMSM under two-phase open-circuit faulty condition shows the asymmetric self- and mutual inductances. The voltage equation can be expressed as (28), where L_α, L_β and $M_{\alpha\beta}$ represent the self-inductances of the α-axis, β-axis and the $\alpha\beta$-axis mutual inductance under faulty condition, respectively.

Post-fault models of DTP-PMSM have been built in this section. Both single- and two-phase open-circuit faults cause asymmetric inductances which can further bring the 2nd harmonic components. Additionally, torque performance which is directly related to the q-axis current deteriorates because of the 2nd harmonic disturbance.

III. CURRENTS UNDER FAULTY CONDITION

The rotation MMF due to the armature windings currents under faulty condition should maintain unchanged as healthy condition to preserve the torque performance, Therefore, the current of faulty phase should be compensated by other healthy phase currents.

The rotation MMF of stator currents under healthy condition can be expressed as:

$$\begin{aligned} F_s &= F_A + F_B + F_C + F_X + F_Y + F_Z \\ &= N\left(i_A e^{j0^\circ} + i_B e^{j120^\circ} + i_C e^{j240^\circ} + i_X e^{j0^\circ} + i_Y e^{j120^\circ} + i_Z e^{j240^\circ}\right) \\ &= NI_m\left(2\cos(\omega t)\, e^{j0^\circ} + 2\cos\left(\omega t - \frac{2\pi}{3}\right)e^{j120^\circ} + 2\cos\left(\omega t - \frac{4\pi}{3}\right)e^{j240^\circ}\right) \\ &= 3NI_m e^{j\omega t} \end{aligned} \tag{19}$$

where ω represents the electrical angular velocity. N and I_m represent the winding turns of each phase and the phase current amplitude, respectively.

The rotation MMF under single-phase fault changes as:

$$\begin{aligned} F_s' &= F_B' + F_C' + F_X' + F_Y' + F_Z' \\ &= N_s \left(i_B' e^{j120^\circ} + i_C' e^{j240^\circ} + i_X' e^{j0^\circ} + i_Y' e^{j120^\circ} + i_Z' e^{j240^\circ} \right) \end{aligned} \tag{20}$$

To make sure that the MMF does not change under faulty condition, the healthy five phase currents should be modified as:

$$i_X' = 2i_m \cos(\omega t) \tag{21}$$

$$i_B' + i_Y' = 2i_m \cos(\omega t - 2\pi/3) \tag{22}$$

$$i_C' + i_Z' = 2i_m \cos(\omega t + 2\pi/3) \tag{23}$$

The relationship explains that the current in phase A is compensated by currents in phase X, since two phases are in phase. Hence, the current in phase X must double to maintain the MMF unchanged.

Similarly, stator currents under two-phase open-circuit fault should be, (24)–(28), as shown at the bottom of the page.

IV. HARMONIC SUPPRESSION METHODS

A. THE FEEDFORWARD COMPENSATION

The 2nd harmonic component is the dominant harmonic component in both single- and two-phase open-circuit faults and it leads to periodic disturbance in the dq-axis currents. The feedforward compensation method was used to compensate the 2nd harmonic component in [17], but it is only suited for five-phase PM motor. Therefore, the feedforward compensation method suitable for DTP-PMSM with 0° phase shifting should be deduced. As shown in (27), the dq-axis voltages under single-phase open-circuit fault are contributed by the DC components and the 2nd harmonic components which can be expressed as:

$$\begin{bmatrix} \Delta u_d \\ \Delta u_q \end{bmatrix} = -\omega \frac{\Delta L}{2} \begin{bmatrix} \sin 2\theta & \cos 2\theta \\ \cos 2\theta & -\sin 2\theta \end{bmatrix} \begin{bmatrix} i_d \\ i_q \end{bmatrix} \tag{29}$$

For motor with two-phase open-circuit fault, the 2nd harmonic components in (28) can be written as (30), shown at the bottom of the page, where $\Delta L_{\alpha\beta} = L_\alpha - L_\beta$.

The 2nd harmonic can be reduced by introducing feedforward compensation term shown in Fig 4. Δu_d and Δu_q acting as the feedforward terms can be added into the reference dq-axis voltages in close loop controller.

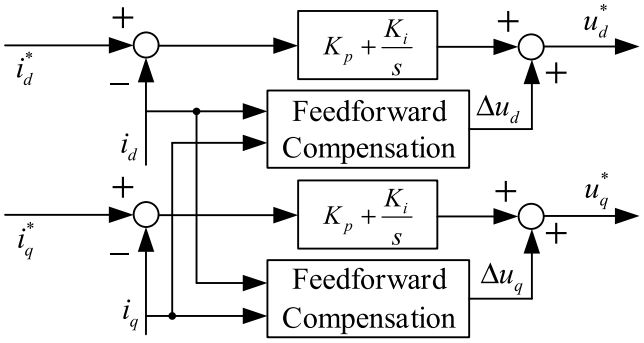

FIGURE 4. Structure of the feedforward compensation controller.

The 2nd harmonic voltages are related to the motor speed ω and asymmetric inductances. Therefore, the accuracy of the feedforward compensation method is influenced by the measured speed and inductance. However, the measured

$$i_X' = 2i_m \cos(\omega t) \tag{24}$$

$$i_Y' = 2i_m \cos(\omega t - 2\pi/3) \tag{25}$$

$$i_C' + i_Z' = 2i_m \cos(\omega t + 2\pi/3) \tag{26}$$

$$\begin{aligned} \begin{bmatrix} u_d \\ u_q \end{bmatrix} &= \begin{bmatrix} L + \Delta L/2 + \Delta L \cos 2\theta/2 & -\Delta L/2 \sin 2\theta \\ -\Delta L/2 \sin 2\theta & L + \Delta L/2 - \Delta L \cos 2\theta/2 \end{bmatrix} \frac{d}{dt} \begin{bmatrix} i_d \\ i_q \end{bmatrix} \\ &+ \omega \begin{bmatrix} -\Delta L/2 \sin 2\theta & -L - \Delta L/2 - \Delta L \cos 2\theta/2 \\ L + \Delta L/2 - \Delta L \cos 2\theta/2 & \Delta L/2 \sin 2\theta \end{bmatrix} \begin{bmatrix} i_d \\ i_q \end{bmatrix} + \begin{bmatrix} R_s & 0 \\ 0 & R_s \end{bmatrix} \begin{bmatrix} i_d \\ i_q \end{bmatrix} + \omega \begin{bmatrix} 0 \\ \psi_{fd} \end{bmatrix} \end{aligned} \tag{27}$$

$$\begin{aligned} \begin{bmatrix} u_d \\ u_q \end{bmatrix} &= \begin{bmatrix} 0.5\left(L_\alpha + L_\beta\right) + 0.5\left(L_\alpha - L_\beta\right)\cos 2\theta + M_{\alpha\beta} \sin 2\theta & -0.5\left(L_\alpha - L_\beta\right)\sin 2\theta + M_{\alpha\beta} \cos 2\theta \\ -0.5\left(L_\alpha - L_\beta\right)\sin 2\theta + M_{\alpha\beta} \cos 2\theta & 0.5\left(L_\alpha + L_\beta\right) - 0.5\left(L_\alpha - L_\beta\right)\cos 2\theta - M_{\alpha\beta} \sin 2\theta \end{bmatrix} \frac{d}{dt} \begin{bmatrix} i_d \\ i_q \end{bmatrix} \\ &+ \begin{bmatrix} R_s & 0 \\ 0 & R_s \end{bmatrix} \begin{bmatrix} i_d \\ i_q \end{bmatrix} \\ &+ \omega \begin{bmatrix} -0.5\left(L_\alpha - L_\beta\right)\sin 2\theta + M_{\alpha\beta} \cos 2\theta & -0.5\left(L_\alpha + L_\beta\right) + 1.5\left(L_\alpha - L_\beta\right)\cos 2\theta - M_{\alpha\beta} \sin 2\theta \\ 0.5\left(L_\alpha + L_\beta\right) + 1.5\left(L_\alpha - L_\beta\right)\cos 2\theta - M_{\alpha\beta} \sin 2\theta & 0.5\left(L_\alpha - L_\beta\right)\sin 2\theta - M_{\alpha\beta} \cos 2\theta \end{bmatrix} \begin{bmatrix} i_d \\ i_q \end{bmatrix} \\ &+ \omega \begin{bmatrix} 0 \\ \psi_{fd} \end{bmatrix} \end{aligned} \tag{28}$$

$$\begin{bmatrix} \Delta u_d \\ \Delta u_q \end{bmatrix} = \omega \begin{bmatrix} -0.5\Delta L_{\alpha\beta} \sin 2\theta + M_{\alpha\beta} \cos 2\theta & 1.5\Delta L_{\alpha\beta} \cos 2\theta - M_{\alpha\beta} \sin 2\theta \\ 1.5\Delta L_{\alpha\beta} \cos 2\theta - M_{\alpha\beta} \sin 2\theta & 0.5\Delta L_{\alpha\beta} \sin 2\theta - M_{\alpha\beta} \cos 2\theta \end{bmatrix} \begin{bmatrix} i_d \\ i_q \end{bmatrix} \tag{30}$$

inductance is commonly inaccurate, which makes the 2nd harmonic currents difficult to compensate completely. Furthermore, the phase of the 2nd harmonic components changes with the different faulty phase, thus the controller requires detecting the faulty phase and then adjust the control algorithm, which increases the complexity of the harmonic suppression method.

B. THE 2nd PIR CONTROLLER

Vector control in healthy condition can decouple the dq-axis flux linkage completely and voltage equation does not obtain the 2nd harmonic component. Therefore, the PI controller can be applied under healthy condition to track the DC components in the dq-axis currents. However, when the dq-axis currents contain specific harmonic components, the PI controller cannot track on and compensate these components in steady state.

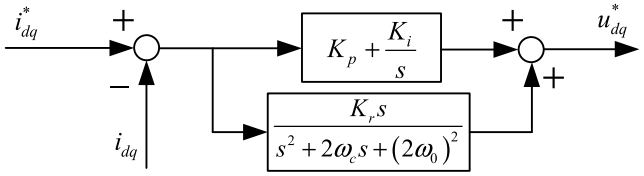

FIGURE 5. Structure of the 2nd PIR controller.

A PIR controller is applied by connecting a resonant controller paralleled with a PI controller to suppress the 2nd disturbance in the dq-axis currents, and the structure of PIR controller is shown in Fig. 5. The transfer function of the ideal resonant controller can be expressed as:

$$G(s) = K_r s \Big/ \left(s^2 + (2\omega_0)^2\right) \tag{31}$$

where K_r is the resonant gain and ω_0 is the electrical angular velocity of rotor.

The ideal resonant controller is difficult to apply in practice due to its narrow bandwidth, which leads to poor frequency robustness [26]. Thus, in this paper, the quasi-resonant controller is introduced and the transfer function is:

$$G(s) = K_r s \Big/ \left(s^2 + 2\omega_c s + (2\omega_0)^2\right) \tag{32}$$

where the ω_c is the cutoff frequency of the resonant controller.

The bode plots of the ideal and quasi-resonant controllers are shown in Fig. 6, where the bandwidth of the quasi-resonant controller is wider than the ideal resonant controller. The resonant controller can produce a gain which is high enough at the resonant frequency to accurately track the sinusoidal signal. Therefore, the PI controller acts as the main controller and can track the DC components in the dq-axis currents. The resonant controller can track and compensate the 2nd harmonic disturbance in the dq-axis currents.

The PIR controller is of high robustness which means that the compensation accuracy is little affected by the change of motor parameters such as inductance. Moreover, different types of fault such as single- and two-phase open-circuit

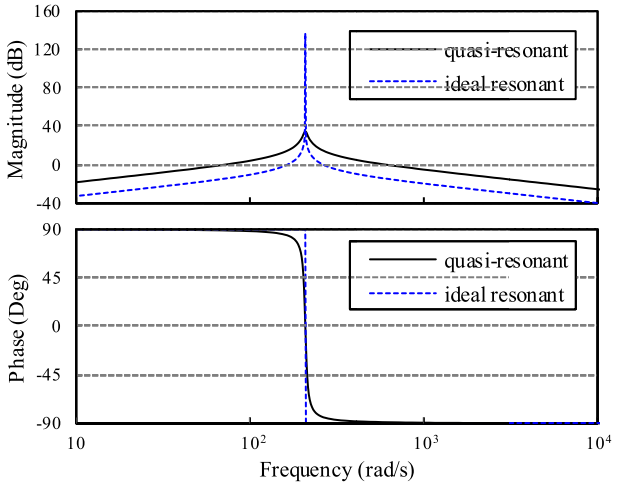

FIGURE 6. Bode plot of two resonant controllers. ($K_r = 100$, $\omega = 33.3 \times 2\pi$ rad/s, $\omega_c = 5$ rad/s).

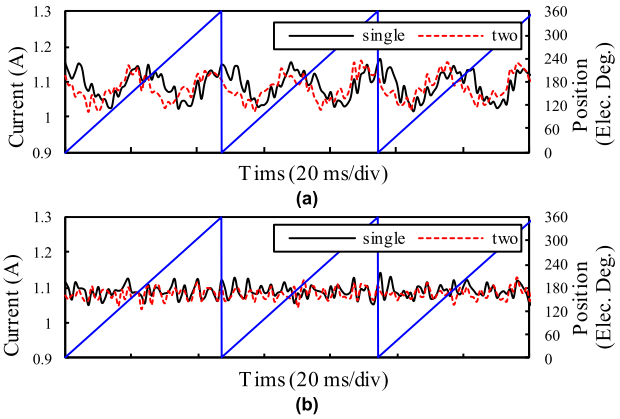

FIGURE 7. Simulation result of the q-axis currents under single- and two-phase faulty conditions. (a) without applying the resonant controller. (b) applying the resonant controller.

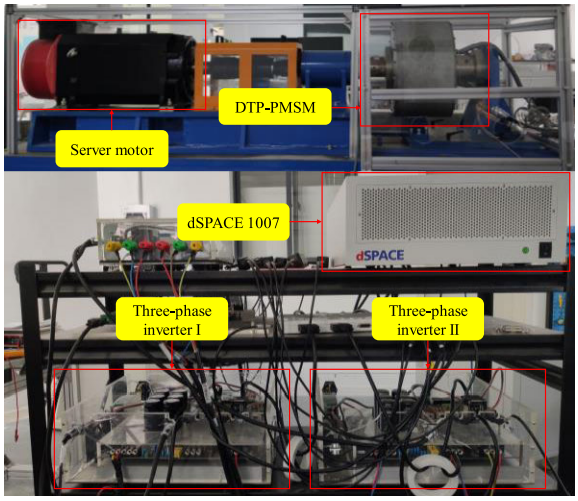

FIGURE 8. Experimental setup.

faults change the phase and amplitude of the 2nd harmonic components. The simulation result is shown in Fig. 7(a). However, the PIR controller with the same parameters can

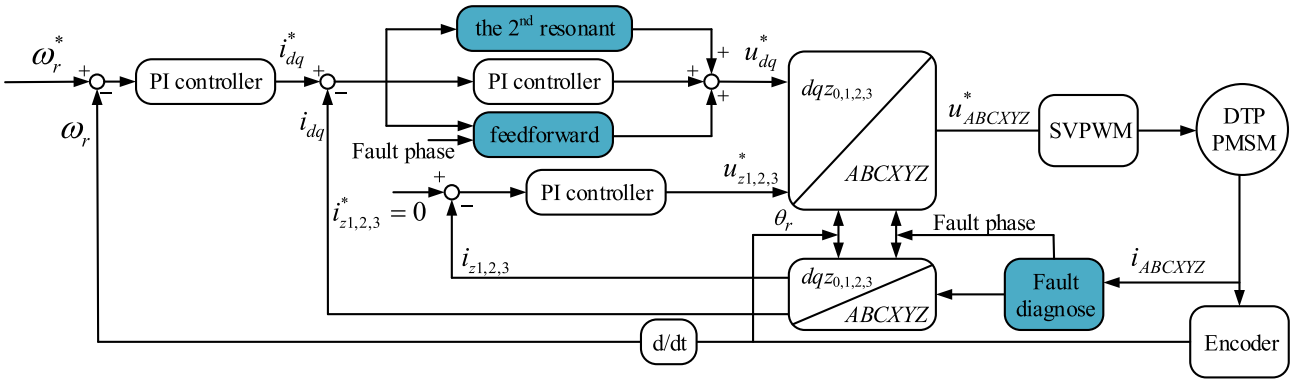

FIGURE 9. Control system schematic.

adapt to both single- and two-phase open-circuit faulty conditions which is shown in Fig. 7(b). Therefore, the PIR controller can cope with different types of fault effectively without modifying fault tolerant control algorithm.

The motor control system schematic is shown in Fig. 9, where θ_r and ω_r represent the rotor electrical angle and electrical speed, respectively.

V. EXPERIMENTAL RESULT

In this paper, a 1.1 kW surface-mounted no-phase-shifting DTP-PMSM is used to verify the fault tolerant control strategy. Fig. 8 shows the prototype of the experimental system. It consists of the prototype machine, two three-phase inverters, one dc power supply and the controller. IGBT modules FP75R12KT4 made by INFINEON are utilized as the power devices and its switching frequency is 10 kHz. The open-circuit fault is achieved by disconnecting the motor phase directly. In the experiment part of this paper, phase *A* is disconnected under single-phase faulty condition. Phases *A* and *B* are disconnected under two-phase faulty condition. The neutral points of two sets of windings are connected directly. The rotor position and speed are measured by Kubler A02H incremental encoder. The fault tolerant control strategy is conducted on dSPACE 1007 controller. The control cycle and sampling period of current, rotor position and speed are 100 μs. The reference of the speed is 80 rpm and the load torque is 50 Nm in the experiments. Design parameters of this motor are listed in TABLE 1.

TABLE 1. Motor design parameters.

Symbol	Parameter	Value
ω_r	rated speed	80 rpm
P_N	rated power	1.1 kW
V_{dc}	DC Voltage	370 V
V_N	rated line-line voltage (RMS)	250 V
I_N	rated current (peak)	3 A
T_N	rated torque	130 Nm
P_r	number of pole pairs	16
ψ_{fm}	PM flux linkage	0.948 Wb
R_s	stator resistance	3 Ω
L_{dq}	*dq*-axis inductance	19.0 mH

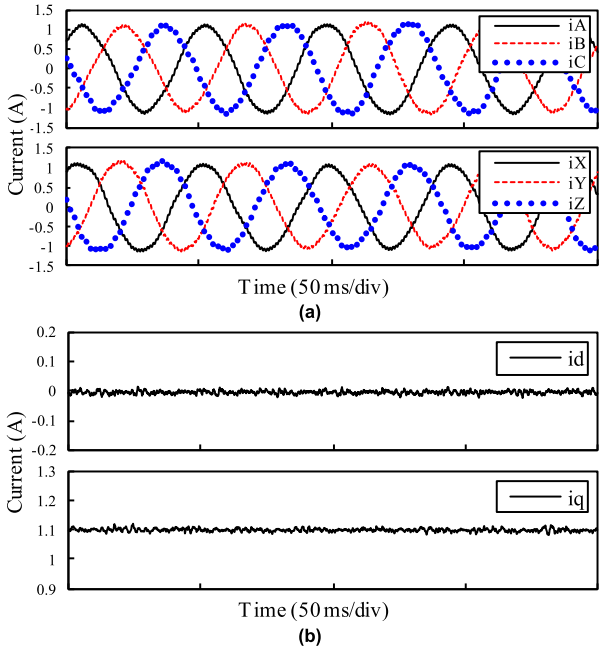

FIGURE 10. Currents under healthy condition. (a) Six-phase stator currents. (b) *do*-axis currents.

A. HEALTHY CONDITION

In order to validate the proposed vector control method, the phase currents and the *dq*-axis currents are provided in Fig. 10. It can be observed in Fig. 10 that the currents of two windings are symmetrical and the amplitude of phase currents is about 1.1 A. Although the phase inductances are asymmetric in single windings, the equivalent three phase PMSM obtains symmetrical equivalent inductance under healthy condition and no obvious harmonic can be observed in the *dq*-axis currents.

B. SINGLE-PHASE FAULTY CONDITION

Fig. 11 shows the currents under single-phase open-circuit faulty condition. The 2nd harmonic can be observed in the

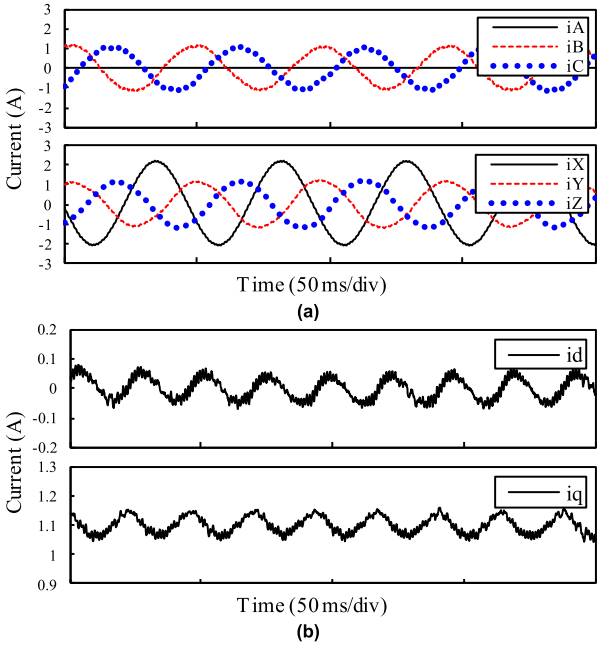

FIGURE 11. Currents under single-phase open-circuit faulty condition. (a) Six phase stator currents. (b) dq-axis currents.

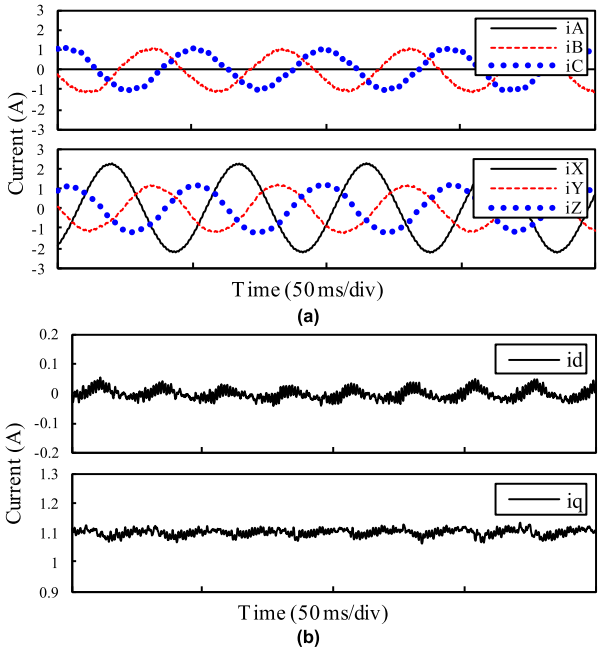

FIGURE 12. Currents applying the feedforward compensation controller under single-phase faulty condition. (a) Six phase stator currents. (b) dq-axis currents.

dq-axis currents. The feedforward compensation and resonant controller are applied to suppress the 2nd current harmonic which are shown in Figs. 12-13. It can be observed that the feedforward compensation can reduce the 2nd harmonic in the *dq*-axis currents. However, it still exists and obvious due to the inaccurate inductance measurement. On the contrary, the resonant controller is much more effective even when the parameters are not accurate.

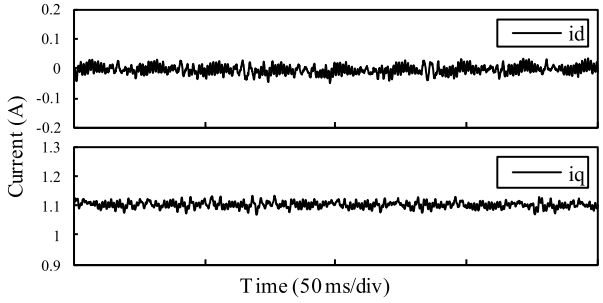

FIGURE 13. *dq*-axis currents applying the 2nd PIR controller under single-phase faulty condition.

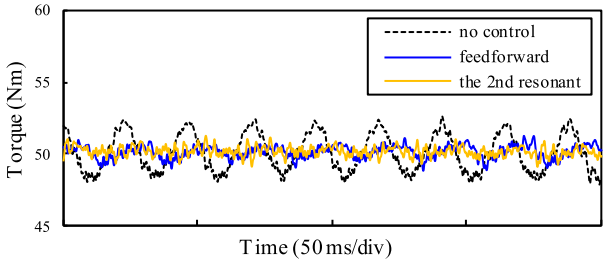

FIGURE 14. Comparison of torque waveforms.

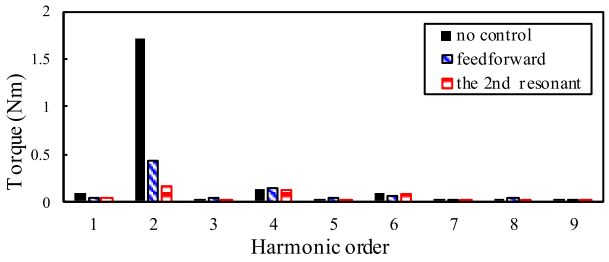

FIGURE 15. Comparison of torque spectra.

Fig. 14 compares the torque waveforms for three cases: without applying harmonic suppression control, with applying the feedforward compensation and with applying the 2nd resonant controller. From the FFT result in Fig. 15, it can be observed that two methods significantly suppress the 2nd harmonic disturbances. However, the resonant controller is preferable for suppression of the 2nd harmonic. The DC component is about 50.1 Nm, and the amplitude of the 2nd harmonic torque is decreased from about 1.72 Nm to 0.43 Nm in the feedforward compensation and to 0.17 Nm in the resonant controller.

C. TWO-PHASE FAULTY CONDITION

Fig. 16 shows the currents under two-phase open-circuit fault. The feedforward compensation controller and resonant controller can be applied to two-phase open-circuit fault. The feedforward terms should be modified because the phase of the 2nd harmonic component is changed compared with the single-phase fault. However, the resonant terms do not

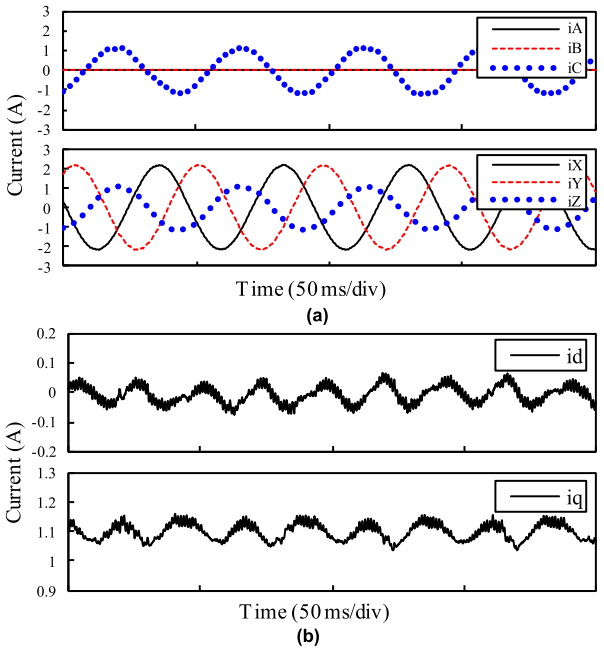

FIGURE 16. Currents under two-phase open-circuit fault. (a) Six phase stator currents. (b) *dq*-axis currents.

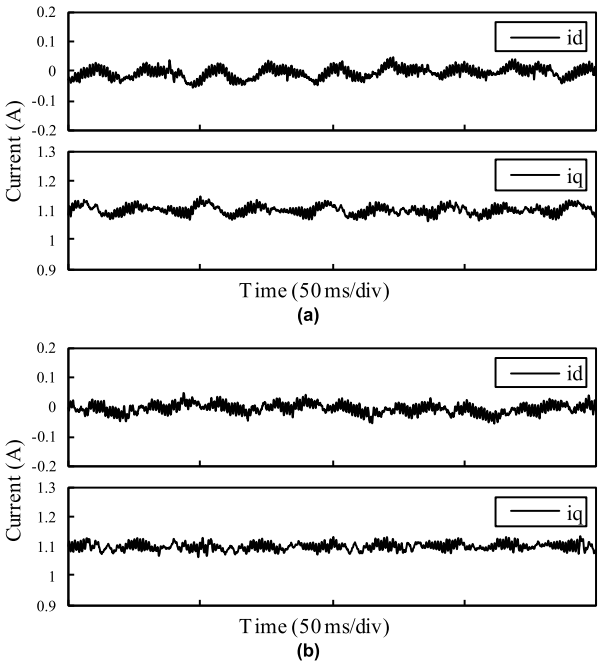

FIGURE 17. *dq*-axis currents applying fault tolerant control under two-phase open circuit fault. (a) the feedforward compensation. (b) the 2nd resonant controller.

need modification. Fig. 17 shows the *dq*-axis currents applying feedforward compensation and the resonant controllers.

Figs. 18 and 19 compare the torque waveforms and spectra for three cases which are the same as Figs. 14-15. The resonant controller is again preferable for suppression of the 2nd harmonic. The 2nd harmonic is about 1.48 Nm under

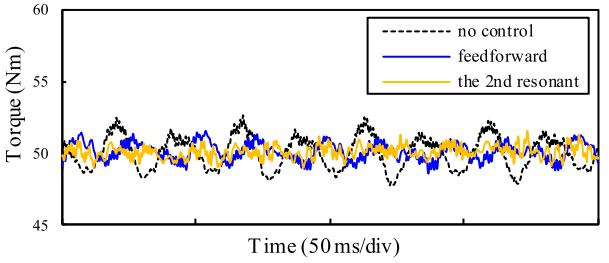

FIGURE 18. Comparison of torque waveforms.

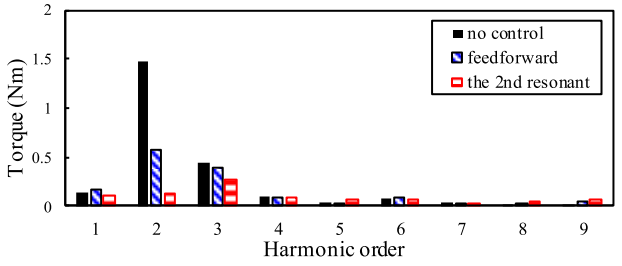

FIGURE 19. Comparison of torque spectra.

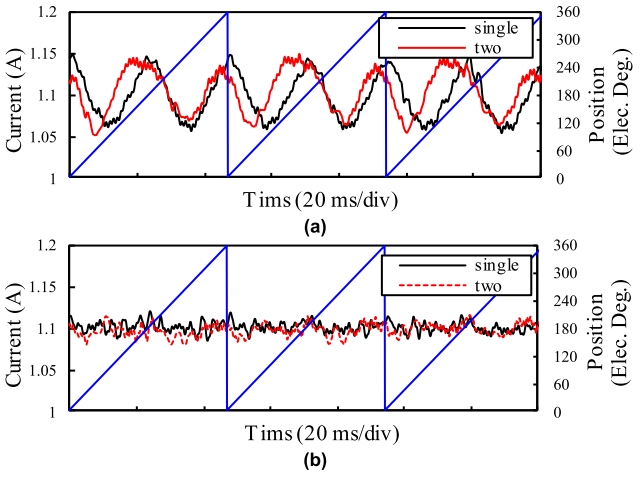

FIGURE 20. *q*-axis currents under single- and two-phase faulty conditions. (a) without applying the resonant controller. (b) applying the resonant controller.

two-phase fault, and it decreases to 0.57 Nm and to 0.14 Nm with applying the feedforward compensation and the resonant controller, respectively.

By comparing these two fault tolerant control methods, we can conclude that the 2nd resonant controller has more advantages which can suppress the 2nd harmonic disturbance better. Meanwhile, self-inductance is difficult to measure precisely and changes with temperature and current value considering core saturation in practice. Hence, the feedforward compensation related to inductance cannot always compensate the harmonic effectively. The experiments validate the robustness of the resonant controller which is less dependent on motor parameters. The 2nd harmonic in the *dq*-axis currents and torque can be suppressed under single- and two-phase open-circuit faulty conditions with the proposed fault-tolerant control method.

The 2nd harmonic components under single- and two-phase open-circuit faults are shown in Fig. 20. The phase and amplitude of the 2nd harmonic components are different in Fig. 20(a). However, the PIR controller with the same parameters can adapt to both single- and two-phase open-circuit faulty conditions which is shown in Fig. 20(b). The q-axis current harmonics in both situations are suppressed effectively which validated the effectiveness of the PIR controller.

VI. CONCLUSION

The paper has proposed a fault tolerant control method for no-phase-shifting DTP-PMSM. The PIR controller is applied in fault tolerant control to suppress the 2nd harmonic disturbance in the dq-axis currents caused by asymmetric inductance. The 2nd harmonic components are analysed by establishing DTP-PMSM post-fault models. Although the 2nd harmonic components are different under single- and two-phase open-circuit faulty conditions, the PIR controller can adapt to both types of fault. The effectiveness of this proposed fault tolerant control strategy is verified by the experiments on a prototype DTP-PMSM system under both single- and two-phase open-circuit faulty conditions.

REFERENCES

[1] M. Barcaro, N. Bianchi, and F. Magnussen, "Six-phase supply feasibility using a PM fractional-slot dual winding machine," *IEEE Trans. Ind. Appl.*, vol. 47, no. 5, pp. 2042–2050, Sep. 2011.
[2] M. Barcaro, N. Bianchi, and F. Magnussen, "Faulty operations of a PM fractional-slot machine with a dual three-phase winding," *IEEE Trans. Ind. Electron.*, vol. 58, no. 9, pp. 3825–3832, Sep. 2011.
[3] N. Erd and A. Binder, "Numerical and analytical analysis of wave harmonics under spatially intermittent feeding," in *Proc. 13th Int. Conf. Electr. Mach. (ICEM)*, Sep. 2018, pp. 297–303.
[4] Y. Demir and M. Aydin, "A novel asymmetric and unconventional stator winding configuration and placement for a dual three-phase surface PM motor," *IEEE Trans. Magn.*, vol. 53, no. 11, pp. 1–5, Nov. 2017.
[5] L. Zhu, L. Wu, J. Liu, and Y. Guo, "Negative sequence current suppression of dual three-phase permanent magnet synchronous machines considering inductance asymmetry," in *Proc. 22nd Int. Conf. Electr. Mach. Syst. (ICEMS)*, Aug. 2019, pp. 1–7.
[6] Y. Zhao and T. A. Lipo, "Space vector PWM control of dual three-phase induction machine using vector space decomposition," *IEEE Trans. Ind. Appl.*, vol. 31, no. 5, pp. 1100–1109, Sep. 1995.
[7] R. Bojoi, M. Lazzari, F. Profumo, and A. Tenconi, "Digital field-oriented control for dual three-phase induction motor drives," *IEEE Trans. Ind. Appl.*, vol. 39, no. 3, pp. 752–760, May/Jun. 2003.
[8] J. Karttunen, S. Kallio, P. Peltoniemi, P. Silventoinen, and O. Pyrhonen, "Decoupled vector control scheme for dual three-phase permanent magnet synchronous machines," *IEEE Trans. Ind. Electron.*, vol. 61, no. 5, pp. 2185–2196, May 2014.
[9] G. K. Singh, K. Nam, and S. K. Lim, "A simple indirect field-oriented control scheme for multiphase induction machine," *IEEE Trans. Ind. Electron.*, vol. 52, no. 4, pp. 1177–1184, Aug. 2005.
[10] Y. Hu, Z. Q. Zhu, and M. Odavic, "Comparison of two-individual current control and vector space decomposition control for dual three-phase PMSM," *IEEE Trans. Ind. Appl.*, vol. 53, no. 5, pp. 4483–4492, Sep./Oct. 2017.
[11] A. Mohammadpour and L. Parsa, "Global fault-tolerant control technique for multiphase permanent-magnet machines," *IEEE Trans. Ind. Appl.*, vol. 51, no. 1, pp. 178–186, Jan./Feb. 2015.
[12] W. Wang, J. Zhang, M. Cheng, and S. Li, "Fault-tolerant control of dual three-phase permanent-magnet synchronous machine drives under open-phase faults," *IEEE Trans. Power Electron.*, vol. 32, no. 3, pp. 2052–2063, Mar. 2017.
[13] Z. Liang, D. Liang, P. Kou, and S. Jia, "Postfault control and harmonic current suppression for a symmetrical dual three-phase SPMSM drive under single-phase open-circuit fault," *IEEE Access*, vol. 8, pp. 67674–67686, 2020.
[14] H. S. Che, M. J. Duran, E. Levi, M. Jones, W.-P. Hew, and N. A. Rahim, "Postfault operation of an asymmetrical six-phase induction machine with single and two isolated neutral points," *IEEE Trans. Power Electron.*, vol. 29, no. 10, pp. 5406–5416, Oct. 2014.
[15] Z. Changpan, T. Wei, S. X. Dong, Z. Zhaoji, Y. Guijie, and S. Jianyong, "Control strategy for dual three-phase PMSM based on reduced order mathematical model under fault condition due to open phases," *J. Eng.*, vol. 2018, no. 13, pp. 489–494, Jan. 2018.
[16] H.-M. Ryu, J.-W. Kim, and S.-K. Sul, "Synchronous-frame current control of multiphase synchronous motor under asymmetric fault condition due to open phases," *IEEE Trans. Ind. Appl.*, vol. 42, no. 4, pp. 1062–1070, Jul./Aug. 2006.
[17] B. Tian, Q.-T. An, J.-D. Duan, D.-Y. Sun, L. Sun, and D. Semenov, "Decoupled modeling and nonlinear speed control for five-phase PM motor under single-phase open fault," *IEEE Trans. Power Electron.*, vol. 32, no. 7, pp. 5473–5486, Jul. 2017.
[18] L. Cheng, Y. Sui, P. Zheng, P. Wang, and F. Wu, "Implementation of post-fault decoupling vector control and mitigation of current ripple for five-phase fault-tolerant PM machine under single-phase open-circuit fault," *IEEE Trans. Power Electron.*, vol. 33, no. 10, pp. 8623–8636, Oct. 2018.
[19] H.-S. Kim, K.-H. Kim, and M.-J. Youn, "On-line dead-time compensation method based on time delay control," *IEEE Trans. Control Syst. Technol.*, vol. 11, no. 2, pp. 279–285, Mar. 2003.
[20] Y. Hu, Z.-Q. Zhu, and K. Liu, "Current control for dual three-phase permanent magnet synchronous motors accounting for current unbalance and harmonics," *IEEE J. Emerg. Sel. Topics Power Electron.*, vol. 2, no. 2, pp. 272–284, Jun. 2014.
[21] G. Feng, C. Lai, W. Li, J. Tjong, and N. C. Kar, "Open-phase fault modeling and optimized fault-tolerant control of dual three-phase permanent magnet synchronous machines," *IEEE Trans. Power Electron.*, vol. 34, no. 11, pp. 11116–11127, Nov. 2019.
[22] Y. Sato, T. Ishizuka, K. Nezu, and T. Kataoka, "A new control strategy for voltage-type PWM rectifiers to realize zero steady-state control error in input current," *IEEE Trans. Ind. Appl.*, vol. 34, no. 3, pp. 480–486, May/Jun. 1998.
[23] A. G. Yepes, F. D. Freijedo, O. Lopez, and J. Doval-Gandoy, "Analysis and design of resonant current controllers for voltage-source converters by means of Nyquist diagrams and sensitivity function," *IEEE Trans. Ind. Electron.*, vol. 58, no. 11, pp. 5231–5250, Nov. 2011.
[24] C. Xia, B. Ji, and Y. Yan, "Smooth speed control for low-speed high-torque permanent-magnet synchronous motor using proportional–integral–resonant controller," *IEEE Trans. Ind. Electron.*, vol. 62, no. 4, pp. 2123–2134, Apr. 2015.
[25] Z. Pan, F. Dong, J. Zhao, L. Wang, H. Wang, and Y. Feng, "Combined resonant controller and two-degree-of-freedom PID controller for PMSLM current harmonics suppression," *IEEE Trans. Ind. Electron.*, vol. 65, no. 9, pp. 7558–7568, Sep. 2018.
[26] Z. Zhou, C. Xia, Y. Yan, Z. Wang, and T. Shi, "Disturbances attenuation of permanent magnet synchronous motor drives using cascaded predictive-integral-resonant controllers," *IEEE Trans. Power Electron.*, vol. 33, no. 2, pp. 1514–1527, Feb. 2018.

ZHUOHANG LI received the B.Eng. degree in electrical engineering from Zhejiang University, Hangzhou, China, in 2018, where he is currently pursuing the master's degree.

His current research interest includes fault tolerant control of multiphase PM motors.

LIJIAN WU (Senior Member, IEEE) received the B.Eng. and M.Sc. degrees in electrical engineering from the Hefei University of Technology, Hefei, China, in 2001 and 2004, respectively, and the Ph.D. degree in electrical engineering from The University of Sheffield, Sheffield, U.K., in 2011.

From 2004 to 2007, he was an Engineer with Delta Electronics (Shanghai) Company Ltd. From 2012 to 2013, he was a Design Engineer with the Sheffield Siemens Wind Power Research Center focusing on wind power generators. From 2013 to 2016, he was an Advanced Engineer with Siemens Wind Power A/S, Denmark. Since 2016, he has been with Zhejiang University, where he is currently a Professor of electrical machines and control systems. His current major research interests include design and control of permanent magnet machines.

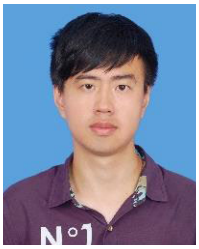

ZEKAI CHEN received the B.Eng. degree in electrical engineering from Zhejiang University, Hangzhou, China, in 2018, where he is currently pursuing the master's degree.

His current major research interest includes control of permanent magnet synchronous motors.

YANG SHI received the B.Eng. degree in engineering mechanics and the Ph.D. degree in hydrodynamics from Zhejiang University, Hangzhou, China, in 2007 and 2012, respectively.

From 2012 to 2017, he was an Engineer with the Shanghai Nuclear Engineering Research and Design Institute. Since 2017, he has been a Research Assistant with Zhejiang University. His current major research interests include cooling design of permanent magnet machines and cooling system design of wind turbines.

LIN QIU (Member, IEEE) received the B.S. and Ph.D. degrees in electrical engineering from the Department of Electrical Engineering, Tsinghua University, in 2011 and 2017, respectively. He is currently a Research Fellow in electrical engineering with Zhejiang University, Hangzhou, China. His current research interests include converter topologies, fintech applications, and cryogentic power converters.

YOUTONG FANG (Senior Member, IEEE) received the B.S. and Ph.D. degrees in electrical engineering from the Hebei University of Technology, Tianjin, China, in 1984 and 2001, respectively. He is currently a Professor with the College of Electrical Engineering, Zhejiang University, Hangzhou, China. His research interests include the application, control, and design of electrical machines.